ISSN 1070-3632, Russian Journal of General Chemistry, 2013, Vol. 83, No. 2, pp. 336–347. © Pleiades Publishing, Ltd., 2013.
Original Russian Text © T.E. Kokina, A.V. Tkachev, L.I. Myachina, S.N. Bizyaev, L.A. Sheludyakova, L.A. Glinskaya, I.V. Korol'kov, E.G. Boguslavskii, S.V. Larionov, 2013, published in Zhurnal Obshchei Khimii, 2013, Vol. 83, No. 2, pp. 282–293.

Synthesis and Structure of Palladium(II) and Copper(II) Complexes with Chiral Bis-α-aminooximes Containing (+)-3-Carene or (+)-Limonene Fragments and 4,4′-Methylenedianiline Linker. Crystal Structure of the Complex $[Cu(i\text{-}PrOH)Cl_2(\mu\text{-}H_2L^3)CuCl_2\cdot H_2O]$

T. E. Kokina[a, b], A. V. Tkachev[b, c], L. I. Myachina[a], S. N. Bizyaev[c], L. A. Sheludyakova[a], L. A. Glinskaya[a], I. V. Korol'kov[a], E. G. Boguslavskii[a], and S. V. Larionov[a]

[a] *Nikolaev Institute of Inorganic Chemistry, Siberian Branch, Russian Academy of Sciences, pr. Akademika Lavrent'eva 3, Novosibirsk, 630090 Russia*
e-mail: kokina@niic.nsc.ru

[b] *Novosibirsk State University, Novosibirsk, Russia*

[c] *Vorozhtsov Novosibirsk Institute of Organic Chemistry, Siberian Branch, Russian Academy of Sciences, pr. Akademika Lavrent'eva 9, Novosibirsk, 630090 Russia*

Received October 4, 2011

Abstract—Coordination compounds $Pd_2(H_2L^2)Cl_4$ (**I**), $Cu_2(H_2L^2)Cl_4$ (**II**), $Pd_2(H_2L^3)Cl_4$ (**III**), and $Cu_2(H_2L^3)Cl_4$ (**IV**), where H_2L^2 and H_2L^3 are chiral bis-α-aminooxime ligands consisting of (+)-3-carene or (+)-limonene fragments and 4,4′-methylenedianiline linker, were synthesized and examined by NMR, ESR, and IR spectroscopy. The structure of $[Cu(i\text{-}PrOH)Cl_2(\mu\text{-}H_2L^3)CuCl_2\cdot H_2O]$ (**V**) was determined by X-ray analysis.

DOI: 10.1134/S1070363213020175

Coordination compounds with optically active ligands derived from natural terpenes attract interest from both theoretical and practical viewpoints [1–4]. We previously synthesized mononuclear Co(II), Co(III), Ni(II), and Cu(II) complexes with chiral ethylenediaminodioximes and propylenediaminodioximes containing fragments of natural terpenes, (+)-3-carene, α-pinene, and limonene [5–13]. We recently reported on the reactions of $PdCl_2$ with chiral ethylenediaminodioxime derived from (+)-3-carene (H_2L) [14] and with *meta*-α,α′-diaminoxylene dioximes derived from (+)-3-carene (H_2L^1), (*R*)-(+)-limonene, and α-pinene [15].

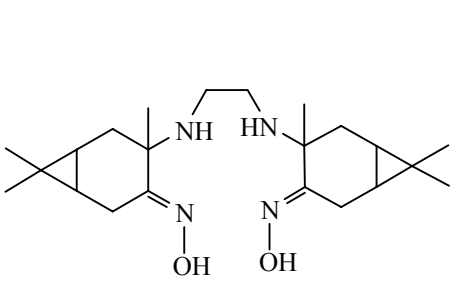

H_2L

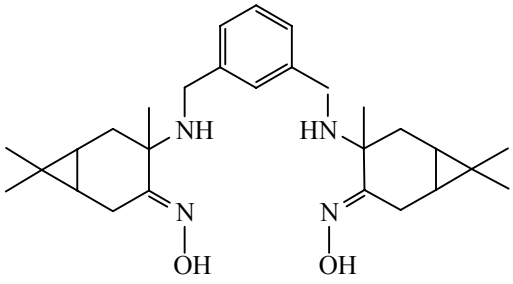

H_2L^1

Unlike H_2L, diaminodioxime H_2L^1 contains a benzene ring in the bridge connecting the terpene fragments. The reactions of these ligands with $PdCl_2$ afforded chiral dinuclear complexes. According to the X-ray diffraction data, the $PdCl_2$ fragments in the complex $[Pd_2(H_2L)Cl_4]$ occupy *trans* positions [14]. Introduction of a benzene ring into the bridge connecting the terpene fragments in H_2L^1 makes that

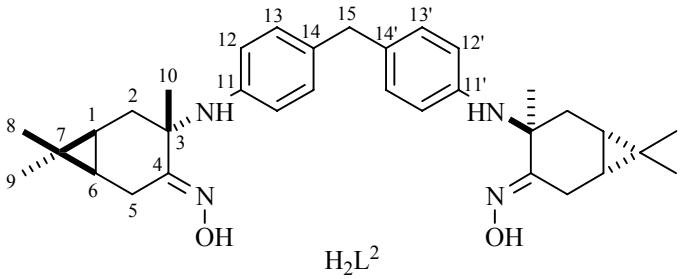

H_2L^2

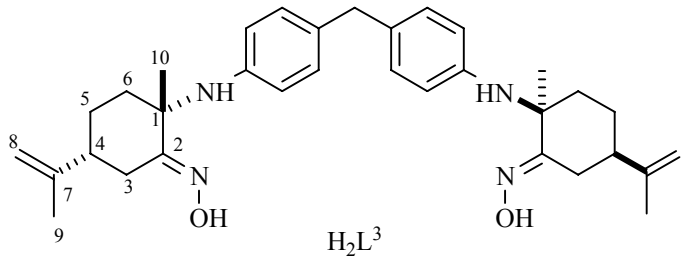

H_2L^3

bridge rigid and fixes cisoid coordination of $PdCl_2$ in the complex $[Pd_2(H_2L^1)Cl_4]$ [15]. It was interesting to examine reactions of $PdCl_2$ and $CuCl_2$ with chiral diaminodioximes in which the bridging moiety between terpene fragments includes two benzene rings.

The goal of the present work was to synthesize Pd(II) and Cu(II) complexes with ligands H_2L^2 (4,4′-methylenebis{*N*-[(1*S*,3*S*,4*E*,6*R*)-4-hydroxyiminocaran-3-yl]-aniline}) and H_2L^3 (4,4′-methylenebis{*N*-[(1*S*,2*E*,4*R*)-2-hydroxyimino-*p*-menth-8-en-1-yl]aniline}) and study their properties.

By reacting palladium(II) and copper(II) chlorides with ligands H_2L^2 and H_2L^3 we obtained compounds **I**–**IV** with a metal–ligand molar ratio of 2:1. In keeping with our previous data [14, 15], this may indicate dinuclear structure of the complexes. Compounds **I** and **III** are diamagnetic, which suggests low-spin (d^8) square configuration of the coordination core. By analogy with $[Pd_2(H_2L)Cl_4]$ [14] and $[Pd_2(H_2L^1)Cl_4]$ [15], complexes **I** and **III** are likely to possess two $PdCl_2N_2$ cores. Like free ligands H_2L^2 and H_2L^3, complexes **I** and **III** are dextrorotatory.

The number of signals in the NMR spectra of **I** is half as much as the number of atoms in molecule H_2L^2 (Table 1); taking into account that the ligand is chiral, this proves C_2 symmetry of the complex. Analysis of spin–spin coupling constants in the spectrum of **I** showed [16] that the six-membered carane ring adopts a slightly distorted boat conformation, which is possible only when a chelate ring is formed with nearly synperiplanar orientation of the amino and oxime nitrogen atoms. Analogous inversion (*half-chair→boat*) of the six-membered carbocycle in 3-substituted caran-4-one oxime derivatives was observed by us previously upon complexation with Ni(II) [5, 7, 13, 17, 18], Co(II) [5], Co(III) [9], Cu(II) [6, 13, 19], and Pd(II) [14, 15]. The five-membered chelate ring PdC_2N_2 is formed *via* coordination of the amino and oxime nitrogen atoms to Pd. The complex formation is not accompanied by hydrogen abstraction from the amino nitrogen atom or oxime oxygen atom, and the corresponding proton signals (N–H and O–H) are retained in the ^{1}H NMR spectrum (the hydroxy proton signal was determined by polarization transfer upon saturation of the HDO signal due to the presence of water traces in CD_3CN, and the N–H signal was identified by ^{15}N–^{1}H coupling).

The configuration of the PdN_2C_2 chelate ring and orientation of the *para*-substituted benzene ring with respect to the cyclohexane ring in the carane fragment were judged by the anomalous upfield shift of the 1-H signal (δ –0.67 ppm in complex **I** against 0.78 ppm in the initial ligand). The only possible reason for the observed shift is the position of the 1-H proton above the aromatic ring plane (due to magnetic susceptibility anisotropy of the latter), which requires in turn *S* configuration of the tetrahedral amino nitrogen atom (*cis* orientation of the methyl group on C^3 and N–H hydrogen atom in the five-membered chelate ring) and coplanar (or nearly coplanar) orientation of the Pd–N(H) bond with respect to the nearest benzene ring (Fig. 1).

Table 1. Parameters of the ^{1}H and ^{13}C NMR spectra of ligand H_2L^2 and complex **I** at 27°C

Atom no.	H_2L^2 (6% in $CDCl_3$)		**I** (5% in CD_3CN)	
	δ_C, ppm	δ_H, ppm (*J*, Hz)	δ_C, ppm	δ_H, ppm (*J*, Hz)
1	16.33	0.78 d.d.d (9.9, 9.8, 4.8)	22.01	–0.67 d.d.d (8.6, 8.5, 8.2)
2	37.65	2.23 d.d (15.2, 9.9), 1.55 d.d (15.2, 4.8)	32.07	1.97 d.d (17.1, 8.2), 1.37 d.d (17.1, 8.5)
3	54.56	–	78.48	–
4	163.72	–	174.30	–
5	18.40	2.04 d.d (17.6, 8.5), 3.08 d.d (17.6, 0.8)	21.34	1.50 d.d (15.8, 8.6), 3.34 d.d (15.8, 8.0)
6	21.39	0.98 d.d.d (9.8, 8.5, 0.8)	22.89	0.70 d.d.d (8.6, 8.6, 8.0)
7	19.44	–	24.44	–
8	14.23	0.84 s	14.23	0.92 s
9	28.06	1.02 s	28.13	0.81 s
10	22.66	1.42 s	30.08	2.04 s
11	144.78	–	142.29[a]	–
12	114.71	6.66 d (8.5)		7.6 br. ($W_{1/2}$ 300 Hz)[c]
13	129.29	6.95 d (8.5)	130.70[b]	7.27 br. ($W_{1/2}$ 22 Hz)[d]
14	131.46	–	141.49[a]	–
15	40.34	3.77 s ($^{1}J_{^{13}C-^{1}H}$ 126.0 Hz)	40.96	3.99 s ($^{1}J_{^{13}C-^{1}H}$ 126.0 Hz)
=N–O<u>H</u>	–	9.34 br.s	–	9.60 br.s
N–<u>H</u>	–	3.99 br.s	–	6.18 s ($^{1}J_{^{15}N-^{1}H}$ 76.1 Hz)

[a] Alternative assignment is possible. [b] The signal in the spectrum recorded with broad-band proton decoupling was appreciably broadened ($W_{1/2}$ = 3.8 Hz) as compared to the other signals ($W_{1/2}$ = 1.2–1.4 Hz). [c] At 50°C: 7.6 br ($W_{1/2}$ = 50 Hz). [d] At 50°C: 7.28 d (8.3).

Presumably, restricted rotation about the C^{14}–C^{15} and C^{15}–$C^{14'}$ bonds does not change its character in going from free ligand H_2L^2 to complex **I**, as follows from slight differences in the spectral parameters of the $ArCH_2Ar$ fragments in H_2L^2 and **I**. Rotation about the N–C^{11} and N′–$C^{11'}$ bonds in molecule H_2L^2 in solution should also be restricted but nevertheless fast on the NMR time scale, which is indicated by narrow signals in the ^{1}H and ^{13}C NMR spectra. Signals from aromatic protons in the ^{1}H NMR spectrum of **I** are strongly broadened, and they become narrower at elevated temperature, their position remaining unchanged. In the ^{13}C NMR spectrum of **I** we observed only one broadened signal from aromatic CH carbon atoms, which was assigned to $C^{13}/C^{13'}$. No $C^{12}/C^{12'}$ signal was detected, presumably because of strong broadening. The observed pattern may be rationalized assuming that the complexation considerably increases the barrier to rotation about the N–C^{11} and N′–$C^{11'}$. As a result, the rate of rotation decreases to a value comparable to the NMR time scale.

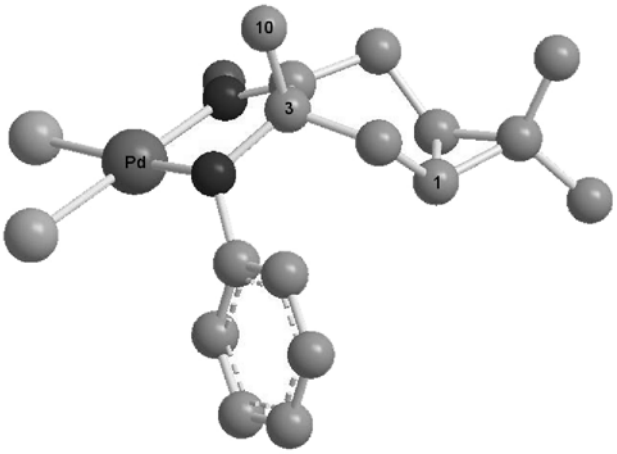

Fig. 1. Partial structure of complex **I** according to the NMR data. One carane fragment with the PdN_2C_2 chelate ring and one benzene ring are shown.

Table 2. Parameters of the ^{1}H and ^{13}C NMR spectra of ligand H_2L^3 and complex **III**

Atom no.	H_2L^3 (5% in $CDCl_3$–DMSO-d_6, 2 : 1 by volume), T = 313 K		**III** (0.5% in $CDCl_3$), T = 293 K	
	δ_C, ppm	δ_H, ppm (J, Hz)	δ_C, ppm	δ_H, ppm (J, Hz)
1	55.88	–	73.62	–
2	161.46	–	170.61	–
3	24.86	*pro-R*: 1.78 d. d (12.2, 12.2) *pro-S*: 3.16 d.d.d (12.2, 3.4, 1.3)	28.84	*pro-R*: 3.47 d.d.d (17.3, 2.2, 2.2) *pro-S*: 2.26 d. d (17.3, 6.0)
4	44.73	[1.99]	37.78	2.47 m ($W_{1/2}$ 13 Hz)
5	25.78	*pro-R*: 1.91 d.d.d. d (12.3, 12.3, 12.3, 3.6) *pro-S*: 1.56 d.m (12.3)	24.53	*pro-R*: 1.91 d.m (14.1, $W_{1/2}$ 9 Hz) *pro-S*: 1.69 d.d.d. d (14.1, 14.1, 4.0, 3.7)
6	42.00	*pro-S*: [1.99] *pro-R*: 1.52 d.d.d (13.3, 13.3, 4.0)	30.55	*pro-S*: 1.44 d.d.d (14.1, 13.4, 4.0) *pro-R*: 1.28 d.d.d (13.4, 3.7, 3.7)
7	147.94	–	145.04	–
8	108.57	H_a: 4.64 br.s H_b: 4.66 br.s	112.24	H_a: 4.71 br.s H_b: 4.95 br.s
9	20.09	1.67 br.s	21.60	1.61 br.s
10	22.53	1.32 s	28.72	2.20 s
11	144.69	–	139.66[a]	–
12	114.32	6.57 d (8.4)	124.40 126.56	7.22 d (6.7) 7.72 d (6.7)
13	128.29	6.76 d (8.4)	129.15 129.60	6.80 d (7.1) 7.17 d (7.1)
14	129.83	–	139.63[a]	–
15	39.17	3.55 s ($^{1}J_{^{13}C–^{1}H}$ 125.7 Hz)	41.20	3.88 s ($^{1}J_{^{13}C–^{1}H}$ 126.1 Hz)
=N–O<u>H</u>	–	10.26 s	–	9.84 s
N–<u>H</u>	–	4.32 br.s	–	7.02 s ($^{1}J_{^{15}N–^{1}H}$ 78.4 Hz)

[a] Alternative assignment is possible.

Complex **III** also displayed in the NMR spectra a halved set of signals with respect to the number of atoms in molecule of H_2L^3 (Table 2) and was assigned C_2 symmetry with account taken of the ligand chirality. Significant downfield shifts of the C^3 and C^4 signals indicated coordination of both amino and oxime nitrogen atoms to palladium.

Analysis of the NMR spectra of free ligand H_2L^3 showed that its molecule, like other structurally related α-amino oximes of the *p*-menthane series [20], exists in a conformation with *chair*-like six-membered carbocycle, equatorial isopropenyl group, and axial amino group on C^1. Comparison of the spectra of ligand H_2L^3 and complex **III** revealed *chair I* → *chair II* type inversion of the six-membered carbocycle as a result of complex formation, so that the isopropenyl group appeared axial, and the C^1–NH group, equatorial. Analogous inversion of *chair*-like conformation of the cyclohexane fragment in 1-amino-*p*-menthan-2-one oximes always accompanies formation of five-membered chelate ring upon coordination to transition metals, which was proved by X-ray analysis of Cu(II) [12, 21, 22], Co(III) [9], Ni(II) [11], and Pd(II) complexes [23]. The six-membered carbocycle in the crystalline complex formed by Pd(II) and piperazine-bridged bis-α-amino oxime of the *p*-menthane series [23] had *twist* conformation which was converted into inverted *chair* upon dissolution in organic solvents. Thus, there are reasons to believe that the five-membered chelate ring in complex **III** is formed *via* coordination of the amino and oxime nitrogen atoms to

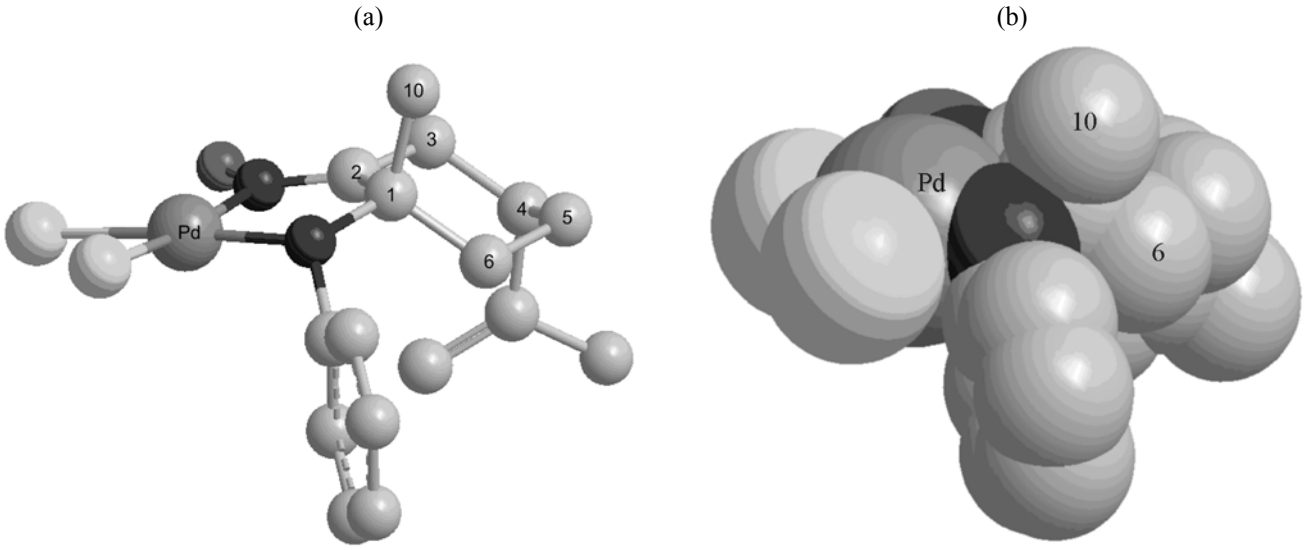

Fig. 2. Partial structure of complex **III** according to the NMR data. (a) Rod-and-ball model and (b) van der Waals radii-based space-filling model. One *p*-menthane fragment, PdN_2C_2 chelate ring, and one benzene ring are shown.

Pd(II) ion and that the ligand remains neutral (neither NH nor oxime OH group undergoes deprotonation). This is confirmed by the presence in the ^{1}H NMR spectrum of **III** of a downfield signal at δ ~10 ppm, which is typical of oximes. The NH signal was identified by the $^1J(^{15}N–^1H)$ coupling constant.

Apart from characteristic variation of spin–spin coupling constants $^3J_{HH}$ due to inversion of the six-membered ring in going from free ligand H_2L^3 to complex **III**, appreciable upfield shift of both 6-H signals and downfield shift of the $C^{10}H_3$ signal were observed in the ^{1}H NMR spectrum of **III**. These shifts indicated quite definitely *S* configuration of the tetrahedral amino nitrogen atom and *trans* orientation of the benzene ring and $C^{10}H_3$ group in the five-membered chelate ring (Fig. 2a). Such structure of the chelate ring is consistent with the anomalous chemical shifts of the 6-H protons (due to shielding by the aromatic ring) and with the aromatic signal pattern. The only possible orientation of the benzene ring, which minimizes non-valence interaction with the neighboring chlorine atom and C^6H_2 methylene group (Fig. 2b), requires that the axial and equatorial protons on C^6 be located above the benzene ring plane and be subject to its strong shielding effect. In contrast, the $C^{10}H_3$ group appears spatially close to the benzene ring plane and is therefore deshielded. The nearest chlorine atom and C^6H_2 methylene group hinder rotation about the N–C^{11} bond so strongly that it becomes slow on the NMR time scale at room temperature. As a result, the $C^{12}H/C^{12'}H$ and $C^{13}H/C^{13'}H$ couples become diastereotopic and distinguishable, giving rise to couples of signals in the NMR spectra. As seen in Fig. 2b, the benzene ring is partly "immersed" into a cavity formed by the chlorine atom and C^6H_2 group, which hampers its rotation about the N–C_{arom} bond. The energy barrier to rotation about that bond was estimated at 15.0±0.5 kcal/mol from the temperature dependence of the width of aromatic proton signals. As follows from the weak differences in the spectral parameters of the $ArCH_2Ar$ fragments in H_2L^3 and **III**, the character of restricted rotation about the C^{14}–C^{15} and C^{15}–$C^{14'}$ bonds therein almost does not change upon complexation.

Thus, according to the NMR data, the reactions of H_2L^2 and H_2L^3 with $PdCl_2$ afforded chiral dinuclear complexes **I** and **III**, respectively, as single C_2-symmetric diastereoisomers with *trans* orientation of the methyl and phenyl groups relative to the five-membered chelate ring. Structural specificities of the terpene fragment in H_2L^3 are responsible for strongly increased (up to 15 kcal/mol) energy barrier to internal rotation about the N–C_{arom} bond.

The ESR spectrum of crystalline compound **II** at liquid nitrogen temperature displayed a single symmetric line with an average *g*-factor value of 2.11 and a width of 160 G. Strong line broadening indicates dinuclear structure of the complex. Crystalline complex **IV** showed an axial spectrum with $g_\parallel = 2.195$ and $g_\perp = 2.074$; line width 55 and 70 G; no hyperfine

Table 3. Principal vibration frequencies (cm^{-1}) in the IR spectra of ligands H_2L^2 and H_2L^3 and complexes **I**–**IV**

Compound no.	ν(OH), ν(NH)	ν(CN)	ν(NO)	ν(M–Cl)
H_2L^2	3327, 3272	1643 sh	928	–
I	3471, 3232, 3108	1650 sh	1027	350,332, 313
II	3441, 3346, 3195	1651 sh	1025	339, 321, 301
H_2L^3	3369, 3269	1645	932	–
III	3475, 3189, 3148	1641	1040	339
IV	3450, 3194, 3168	1641 s	1031	324, 310, 296

structure. The ratio of the longitudinal and transverse *g*-factor shifts (relative to the *g*-factor of free electron) for complex **IV** is 2.6, which is appreciably lower than the value typical of isolated Cu^{2+} ion. These data indicate such crystalline structure of complex **IV** where exchange interaction over magnetically concentrated phase leads to averaged spectrum. In addition, non-coaxial arrangement of the copper(II) coordination polyhedrons in the crystalline structure of **IV** should be assumed.

The ESR spectra of frozen solutions of **II** and **IV** in $CHCl_3$ resemble the solid-phase spectrum of **II**. This suggests that complexes **II** and **IV** have dinuclear structure in solution as well. Complex **IV** is likely to be dinuclear in crystal.

The experimental effective magnetic moments μ_{eff} of paramagnetic complexes **II** (2.56 B.M.) and **IV** (2.52 B.M.) are close to the calculated value (2.58 B. M.) for a system of two magnetically non-interacting Cu^{2+} ions at 300 K provided that $g = 2.11$.

The IR spectra of ligands H_2L^2 and H_2L^3 and complexes **I**–**IV** are generally similar in the regions corresponding to their main functional groups [ν (C=N), ν(N–O), ν(NH), ν(OH); Table 3]. In the spectra of **I**–**IV** the ν(N–O) band is displaced to higher frequencies, and the ν(C=N), ν(NH), and ν(OH) bands also change their position relative to analogous bands in the spectra of the free ligands, which is indicative of coordination at the nitrogen atoms of the amino and oxime groups. Unlike free ligands, the low-frequency region of the IR spectra of **I** and **III** contained new strong ν(Pd–Cl) bands (Table 3); their position was similar to that in the spectrum of analogous complex $[Pd_2(H_2L)Cl_4]$ whose structure was determined in [14]. Comparison of the IR spectra of **II** and **IV** with those of the complex $[Cu(HL^4)Cl_2]$ (where HL^4 is a caryophyllane type α-alkylamino oxime and the coordination entity $CuCl_2N_2$ is a distorted square) [24] allowed us to identify ν(Cu–Cl) bands. According to the IR and Raman spectra, ν(Cu–Cl) stretching vibrations in $[Cu(HL^4)Cl_2]$ give rise to a structured band in the region 317–290 cm^{-1} with its maximum at 305 cm^{-1} [24]. Analogous structured band was observed in the region 339–296 cm^{-1} in the spectra of **II** and **IV**. It was difficult to identify bands due to vibrations of M–N bonds (M = Pd, Cu) in the 500–350-cm^{-1} region of the spectra of **I**–**IV**, for that region also contained absorption bands typical of free ligands H_2L^2 and H_2L^3. In keeping with the IR data, PdN_2Cl_2 coordination core may be presumed for complexes **I** and **III**, and CuN_2Cl_2, for **II** and **IV**.

When the reaction of H_2L^3 with $CuCl_2 \cdot 2H_2O$ was carried out at lower reactant concentrations, we isolated single crystals of the complex $[Cu(i\text{-}PrOH)Cl_2(\mu\text{-}H_2L^3)CuCl_2 \cdot H_2O]$ (**V**) whose composition differed from that of **IV**. The structure of **V** was determined by X-ray analysis. Its crystallographic parameters and details of the X-ray diffraction experiment and structure refinement are given in Table 4. The crystalline structure of **V** is represented by molecules of dinuclear copper(II) complex and crystal water (Fig. 3). Molecule H_2L^3 is a tetradentate bridging and chelating ligand. Coordination of four nitrogen atoms in the ligand molecule to two copper ions leads to closure of two five-membered chelate rings CuN_2C_2. The distances from the copper atoms to the oxime nitrogen atoms [Cu–N 1.993(7)–1.989(7) Å] are appreciably shorter than to the amino nitrogen atoms [2.042(7)–2.052(6) Å] (Table 5). In addition, the oxime groups are involved in intramolecular O–H···Cl hydrogen bonding to form two five-membered H-chelate rings $Cu^1N^2O^1H^{O1}Cl^1$ and $Cu^{2'}N^{2'}O^{1'}H^{O1'}Cl^{1'}$. The $O^1\cdots Cl^1$ and $O^{1'}\cdots Cl^{1'}$ distances are 3.099(7) and

Table 4. Crystallographic parameters of complex **V** and details of X-ray diffraction experiment and structure refinement

Parameter	Value
Formula	$C_{36}H_{52}Cl_4Cu_2N_4O_4$
Molecular weight	873.70
Crystal system	Rombic
Space group	$P\,2_12_12_1$
a, Å b, Å c, Å	8.625(5) 18.957(12) 25.968(16)
V, Å^3	4246(4)
d_{calc}, mg/cm^3; Z	1.367; 4
μ, mm^{-1}	1.293
Crystal size, mm	0.2×0.05×0.05
Scan range θ, deg	1.33–26.52
Total reflection number Number of independent reflections R_{int}	37993 8745 0.1657
Number of reflections with $I > 2\sigma(I)$	8745
Number of refined parameters	482
Goodness of fit (F^2)	0.983
Divergence factor [$I > 2\sigma(I)$] R_1 wR_2	 0.0746 0.1231
Divergence factor (all reflections) R_1 wR_2	 0.2047 0.1593
Absolute structure parameter	–0.02(2)
Residual electron density (max/min), e/Å^3	0.415/–0.398

3.017(7) Å, respectively. Both H-chelate rings have *envelope* conformation where Cl^1 and $Cl^{1'}$ deviate from the $Cu^1N^2O^1H^{O1}$ and $Cu^{2'}N^{2'}O^{1'}H^{O1'}$ planes, respectively, by 0.67(1) and –0.48(1) Å; the hydrogen bond angles are $\angle O^1H^{O1}Cl^1$ 135.0° and $\angle O^{1'}H^{O1'}Cl^{1'}$ 137.5°. Both six-membered carbocycles appear in *chair* conformation: the C^1, C^4 and $C^{1'}$, $C^{4'}$ atoms deviate from the planes formed by the remaining four atoms by –0.57(1), 0.71(1) and 0.55(1), –0.69(1) Å, respectively.

Structure **V** features different coordination numbers (4 and 5) of the copper atoms (Fig. 3). The Cu^1 coordination polyhedron Cl_2N_2 is a distorted tetrahedron formed by two nitrogen atoms of ligand H_2L^3 and two chlorine atoms Cl [Cu–Cl 2.215(2), 2.258(3) Å]. The Cu^2 coordination polyhedron Cl_2N_2O is a distorted square pyramid whose base is formed by two nitrogen atoms of the ligand and two chlorine atoms [Cu–Cl 2.232(3), 2.277(3) Å], and the vertex is occupied by the oxygen atom O^2 of *i*-PrOH molecule as extra ligand. The Cu^2 atom is displaced toward the vertex by 0.224(3) Å. The Cu^2–O^2 distance equal to 2.267(8) Å only slightly differs from the Cu–O distance (2.213 Å) in the copper(II) complex containing a coordinated MeOH molecule [25]. Thus we have revealed the possibility for coordination of *i*-PrOH molecule in the reaction of $CuCl_2 \cdot 2H_2O$ with H_2L^3 in *i*-PrOH–MeCN. Presumably, complex **IV** contained neither crystal water nor *i*-PrOH molecules since the product was dried in a vacuum desiccator over anhydrous magnesium perchlorate. The $CuCl_2$ fragments in structure **V** appear in a *cisoid* arrangement. The Cu^1–N^1 and $N^{1'}$–Cu^2 bonds together with the $N^1\cdots C^{15}$ and $C^{15}\cdots N^{1'}$ axes form a *W*-shaped profile (the $Cu^1N^1C^{15}$, $N^1C^{15}N^{1'}$, and $C^{15}N^{1'}Cu^2$ angles are 105.2, 116.9, and 103.8°, respectively; Fig. 3). The N_2Cl_2 planes in the coordination units are turned through a dihedral angle of ~49.3° with respect to each other. The $Cu^1\cdots Cu^2$ distance is 4.470(4) Å.

Figure 4 shows projection of the crystalline structure of complex **V** onto the (100) plane. Analysis of intermolecular distances in structure **V** revealed additional contacts between the Cu^1 atom of one molecule and Cl^2 atom in the neighboring molecule [2.983(4) Å], as well as other contacts and hydrogen bonds involving chlorine atoms (Fig. 4). The $Cu^1\cdots Cl^2$ distance is considerably longer than the Cu–Cl coordination bond in compounds with one bridging chlorine atom (2.51–2.67 Å) [22, 26]; therefore, it may be regarded as a contact. The shortest contacts formed by chlorine atoms are $Cl^1\cdots O^2$ 3.130(9) Å and $Cl^2\cdots N^{1'}$ 3.377(8) Å. These contacts link dinuclear molecules **V** to produce zigzag chains along the *c* axis. Disordered crystal water molecules are located between molecules **V** and are also involved in hydrogen bonding.

The structure of complex **III** assigned on the basis of its NMR spectra is similar to the structure of **V** determined by X-ray analysis. Complexes **III** and **V** are characterized by similar *chair*-like conformations of the six-membered carbocycle with equatorial isopropenyl group and axial NH group on C^1, *trans*

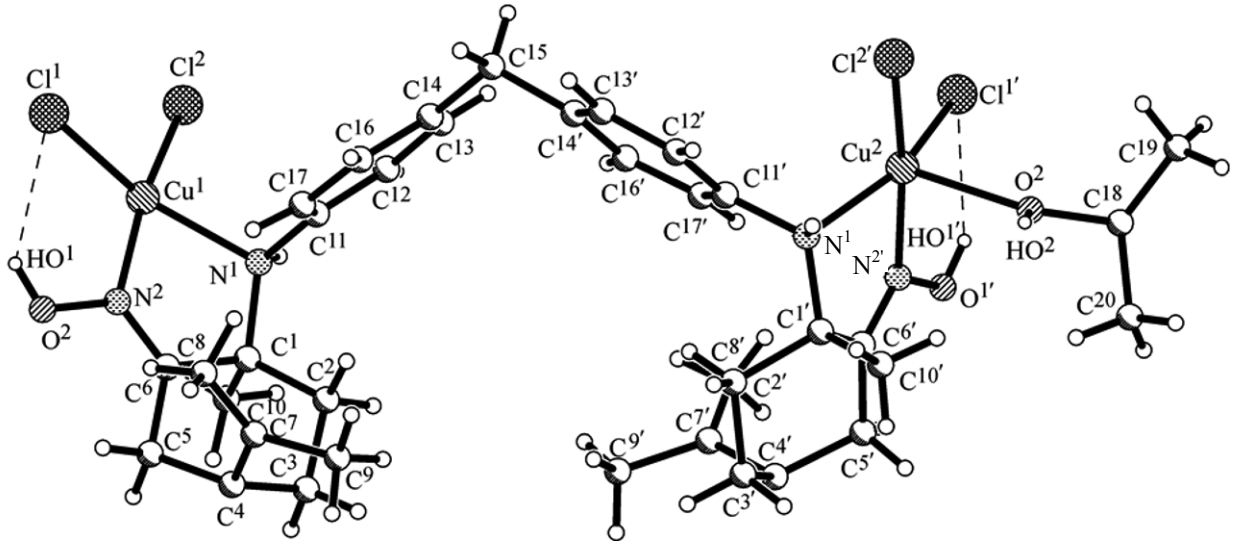

Fig. 3. Structure of acentric dinuclear complex **V** according to the X-ray diffraction data. Numbering of non-hydrogen atom is given.

orientation of the methyl and phenyl groups in the five-membered chelate ring, and partial insertion of the benzene ring into the cavity formed by the chlorine atom in the neighboring coordination unit and C^6H_2 group.

Thus the results of the present study have extended the series of dinuclear Pd(II) complexes with chiral diamino dioximes derived from natural terpenes, and demonstrated the possibility for the preparation of analogous dinuclear Cu(II) complexes.

EXPERIMENTAL

The elemental compositions were determined on Hewlett–Packard 185, Carlo Erba 1106, and Euro EA 3000 analyzers. The magnetic susceptibilities of polycrystalline complexes were measured by the Faraday method at room temperature. The ESR spectra of **II** and **IV** were recorded on a Varian E-109 radiospectrometer equipped with an analog-to-digital converter and proprietary software for data acquisition and primary processing. The spectra were recorded in the *Q*-range at room temperature and in the *X*-range at liquid nitrogen temperature (frozen solutions with a concentration of 10^{-2} to 10^{-3} M) using MgO powder containing Mn^{2+} ions at a ratio of 1:5000 (g = 2.003, a = 86.8 G) or 2,2-diphenyl-1-picrylhydrazyl as calibration standard. The NMR spectra were obtained on a Bruker DRX-500 instrument at 500.13 MHz for ^1H and 125.75 MHz for ^{13}C at 27 and 50°C. The chemical shifts were determined relative to the solvent signals ($CHCl_3$, δ 7.24 ppm; $CDCl_3$, δ_C 76.90 ppm; CHD_2CN, δ 1.93 ppm; CD_3CN, δ_C 118.20 ppm). Signals were assigned using *J*-modulation (noise-modulated proton decoupling, opposite phase for CH_2 protons, adjustment for a direct coupling constant $^1J_{CH}$ of 145 Hz) and two-dimensional homo (^1H–^1H) and heteronuclear (^{13}C–^1H, J = 145 Hz) correlation techniques. The internal rotation barrier $\Delta G^{\neq}$ (kcal/mol) was estimated by the Eyring equation on the basis of the temperature dependence of the aromatic proton signal width. The IR spectra were obtained in the range from 4000 to 200 cm^{-1} on Scimitar FTS 2000, BOMEM MB-102, and Bruker TENSOR 27 spectrometers with Fourier transform; samples were prepared as mulls in mineral or fluorinated oil, KBr or CsI pellets, or 1% solutions in $CHCl_3$. The optical rotations were measured on a PolAAr 3005 polarimeter. The mass spectra (electron impact, 70 eV) were recorded on a Thermo Scientific DFS mass spectrometer.

The X-ray diffraction data for a single crystal of **V** were acquired on a Bruker X8 Apex CCD automatic diffractometer equipped with a two-coordinate detector (MoK_α irradiation, λ = 0.71073 Å, graphite monochromator) according to standard procedure. The structure was solved by the direct method and was refined against F^2 by the full-matrix least-squares procedure in anisotropic approximation for non-hydrogen atoms using SHELXL-97 software package [28]. Hydrogen atoms were placed into positions calculated on the basis of geometry considerations and were refined according to the *riding* model. Hydrogen atoms in crystal water molecules were not localized.

Table 5. Principal bond lengths (*d*) and bond angles (ω) in the crystal structure of **V**[a]

Bond	*d*, Å	Bond	*d*, Å	Bond	*d*, Å	Bond	*d*, Å
$Cu^1–N^2$	1.989(7)	$Cu^2–N^{2'}$	1.993(7)	$N^2–C^6$	1.265(10)	$N^{1'}–C^{1'}$	1.505(9)
$Cu^1–N^1$	2.042(7)	$Cu^2–N^{1'}$	2.052(6)	$C^1–C^{10}$	1.511(11)	$N^{2'}–C^{6'}$	1.254(10)
$Cu^1–Cl^2$	2.215(2)	$Cu^2–Cl^{2'}$	2.232(3)	$C^7–C^8$	1.326(13)	$C^{1'}–C^{10'}$	1.527(11)
$Cu^1–Cl^1$	2.258(3)	$Cu^2–O^2$	2.267(8)	$C^7–C^9$	1.479(13)	$C^{7'}–C^{8'}$	1.353(14)
$O^1–N^2$	1.376(9)	$Cu^2–Cl^{1'}$	2.277(3)	$C^{18}–C^{19}$	1.501(18)	$C^{7'}–C^{9'}$	1.478(14)
$N^1–C^{11}$	1.443(10)	$O^{1'}–N^{2'}$	1.394(9)	$C^{18}–C^{20}$	1.553(17)	$O^2–C^{18}$	1.483(14)
$N^1–C^1$	1.516(10)	$N^{1'}–C^{11'}$	1.468(9)				
Angle	ω, deg	Angle	ω, deg	Angle	ω, deg	Angle	ω, deg
$N^2Cu^1N^1$	78.7(3)	$N^{2'}Cu^2N^{1'}$	77.8(3)	$C^4C^3C^2$	111.4(8)	$C^{6'}C^{1'}C^{2'}$	110.1(7)
$N^2Cu^1Cl^2$	166.4(2)	$N^{2'}Cu^2Cl^{2'}$	169.3(2)	$C^7C^4C^3$	113.5(9)	$N^{1'}C^{1'}C^{2'}$	111.2(7)
$N^1Cu^1Cl^2$	92.3(2)	$N^{1'}Cu^2Cl^{2'}$	91.9(2)	$C^7C^4C^5$	114.5(9)	$C^{10'}C^{1'}C^{2'}$	108.5(8)
$N^2Cu^1Cl^1$	92.9(2)	$N^{2'}Cu^2O^2$	90.1(3)	$C^3C^4C^5$	108.9(9)	$C^{3'}C^{2'}C^{1'}$	111.6(9)
$N^1Cu^1Cl^1$	149.3(2)	$N^{1'}Cu^2O^2$	106.2(3)	$C^6C^5C^4$	110.1(8)	$C^{4'}C^{3'}C^{2'}$	112.6(7)
$Cl^2Cu^1Cl^1$	99.92(11)	$Cl^{2'}Cu^2O^2$	89.8(2)	$N^2C^6C^5$	125.1(9)	$C^{7'}C^{4'}C^{5'}$	115.1(9)
$C^{11}N^1C^1$	118.7(6)	$N^{2'}Cu^2Cl^{1'}$	90.9(2)	$N^2C^6C^1$	116.6(8)	$C^{7'}C^{4'}C^{3'}$	111.5(10)
$C^{11}N^1Cu^1$	104.8(5)	$N^{1'}Cu^2Cl^{1'}$	152.7(2)	$C^5C^6C^1$	118.2(8)	$C^{5'}C^{4'}C^{3'}$	108.0(8)
$C^1N^1Cu^1$	111.6(5)	$Cl^{2'}Cu^2Cl^{1'}$	99.72(11)	$C^8C^7C^4$	125.4(10)	$C^{6'}C^{5'}C^{4'}$	112.7(8)
$C^6N^2O^1$	117.5(8)	$O^2Cu^2Cl^{1'}$	98.4(2)	$C^8C^7C^9$	118.8(9)	$N^{2'}C^{6'}C^{5'}$	127.5(9)
$C^6N^2Cu^1$	119.7(6)	$C^{11'}N^{1'}C^{1'}$	119.5(6)	$C^4C^7C^9$	115.8(9)	$N^{2'}C^{6'}C^{1'}$	112.6(7)
$O^1N^2Cu^1$	122.6(6)	$C^{11'}N^{1'}Cu^2$	104.6(4)	$C^{13}C^{14}C^{15}$	123.3(9)	$C^{5'}C^{6'}C^{1'}$	119.7(8)
$C^{10}C^1N^1$	106.4(7)	$C^{1'}N^{1'}Cu^2$	109.0(5)	$C^{16}C^{14}C^{15}$	119.8(9)	$C^{8'}C^{7'}C^{9'}$	117.2(12)
$C^{10}C^1C^2$	113.5(8)	$C^{6'}N^{2'}O^{1'}$	115.0(7)	$C^{14'}C^{15}C^{14}$	115.8(7)	$C^{8'}C^{7'}C^{4'}$	121.8(11)
$N^1C^1C^2$	112.8(7)	$C^{6'}N^{2'}Cu^2$	122.3(6)	$C^{18}O^2Cu^2$	135.7(10)	$C^{9'}C^{7'}C^{4'}$	120.8(11)
$C^{10}C^1C^6$	108.2(7)	$O^{1'}N^{2'}Cu^2$	122.4(6)	$O^2C^{18}C^{19}$	107.5(17)	$C^{17'}C^{11'}C^{12'}$	119.4(8)
$N^1C^1C^6$	105.7(7)	$C^{6'}C^{1'}N^{1'}$	109.6(6)	$O^2C^{18}C^{20}$	96.4(14)	$C^{17'}C^{11'}N^{1'}$	121.3(8)
$C^2C^1C^6$	109.8(8)	$C^{6'}C^{1'}C^{10'}$	109.9(7)	$C^{19}C^{18}C^{20}$	137(2)	$C^{12'}C^{11'}N^{1'}$	119.3(7)
$C^3C^2C^1$	113.3(8)	$N^{1'}C^{1'}C^{10'}$	107.4(7)				

[a] The C–C bond lengths in the benzene rings range from 1.345(10) to 1.403(11) Å, and in the cyclohexane rings, from 1.473(11) to 1.553(11) Å.

The principal bond lengths and bond angles are given in Table 5. The complete set of crystallographic data (including coordinates of atoms, bond lengths, and bond angles) was deposited to the Cambridge Crystallographic Data Centre (entry no. CCDC 840633).

Reagent-grade $CuCl_2 \cdot 2H_2O$ and $PdCl_2$, 96% EtOH, concentrated hydrochloric acid, chemically pure *i*-PrOH, and analytical grade MeCN were used. The ligands H_2L^2 and H_2L^3 were synthesized from 4,4′-methylenedianiline and (+)-3-carene or (+)-limonene, respectively, through the corresponding nitroso

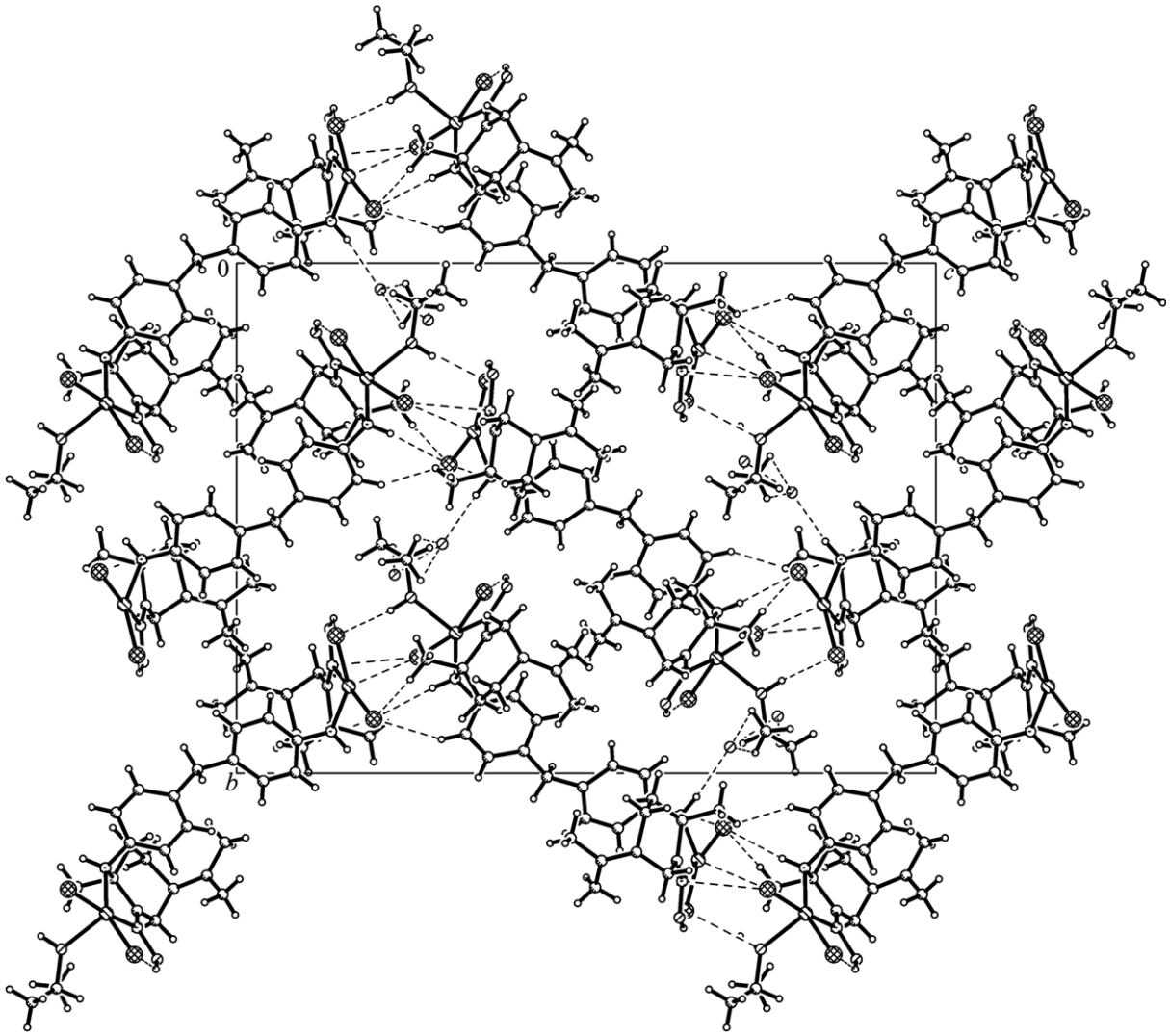

Fig. 4. Projection of the crystal structure of complex **V** onto the (100) plane. Hydrogen bonds and intermolecular contacts are shown with dashed lines.

chlorides according to the procedure described in [3, 27] for the preparation of simplest bis-α-amino oximes.

4,4′-Methylenebis{*N*-[(1*S*,3*S*,4*E*,6*R*)-4-hydroxyiminocaran-3-yl]aniline} (H_2L^2). Grayish–yellowish powder, mp 170–171°C (decomp., from MeCN), $[\alpha]_D^{28}$ = +116 (*c* = 0.56, THF–MeOH, 1:1 by volume). IR spectrum ($CHCl_3$), ν, cm^{-1}: 3586 (O–H), 3422 (N–H), 1615, 940 and 923 (N–O). UV spectrum (EtOH), λ_{max}, nm (logε): 259 (4.18), 299 (3.27). High-resolution mass spectrum: *m*/*z* 528.3455 $[M]^+$. $C_{33}H_{44}N_4O_2$. Calculated: *M* 528.3459. Mass spectrum, *m*/*z* (I_{rel}, %): 528 (1), 363 (19), 346 (10), 345 (5), 305 (5), 281 (16), 238 (6), 223 (19), 198 (51), 197 (33), 182 (15), 180 (12), 165 (30), 150 (53), 148 (22), 135 (20), 133 (15), 132 (26), 123 (42), 122 (26), 119 (10), 118 (11), 110 (30), 107 (29), 106 (100), 105 (40), 94 (21), 93 (37), 91 (77), 79 (51), 77 (70), 67 (33), 65 (26), 55 (26), 53 (29), 51 (16). The NMR spectra are given in Table 1.

4,4′-Methylenebis{*N*-[(1*S*,2*E*,4*R*)-2-hydroxyimino-*p*-menth-8-en-1-yl]aniline} (H_2L^3). Grayish–yellowish powder, mp 145–146°C (decomp., from MeCN), $[\alpha]_D^{28}$ = +49 (*c* = 1.01, MeOH). IR spectrum ($CHCl_3$), ν, cm^{-1}: 3586 (O–H), 3372 (N–H), 3093 (C=CH_2), 1648 (C=N), 1612, 928 (N–O), 893 (C=CH_2). UV spectrum (EtOH), λ_{max}, nm (logε): 258 (4.12), 300 (3.29). High-resolution mass spectrum: *m*/*z* 528.3459 $[M]^+$. $C_{33}H_{44}N_4O_2$. Calculated: *M* 528.3459. Mass spectrum, *m*/*z* (I_{rel}, %): 528 (0.1), 363 (9), 348 (3), 346 (4), 332 (1), 223 (2), 198 (100), 197 (63), 195 (5), 182 (18), 180

(14), 165 (9), 150 (6), 148 (9), 122 (13), 106 (34), 99 (6), 93 (8), 91 (10), 77 (10), 67 (9), 55 (5), 53 (6). The NMR spectra are given in Table 2.

Tetrachloro-μ-(4,4′-methylenebis{*N*-[(1*S*,3*S*,4*E*,6*R*)-4-hydroxyiminocaran-3-yl]aniline}-*N*,*N*,*N*′,*N*′)dipalladium(II) $Pd_2(H_2L^2)Cl_4$ (I). A solution of 0.036 g (0.2 mmol) of $PdCl_2$ in 1.5 ml of concentrated hydrochloric acid was evaporated almost to dryness, 1.5 ml of EtOH was added, and a warm (~50–60°C) solution of 0.053 g (0.1 mmol) of H_2L^2 in 1.5 ml of EtOH was added. A yellow solid separated, the mixture was kept for 3–4 h, and the precipitate was filtered off with suction, washed with EtOH and hexane, and dried in air. Yield 0.050 g (57 %). $[\alpha]_{578}^{20}$ = +78 (*c* = 0.38, CH_2Cl_2). Found, %: C 45.1; H 5.2; N 6.5. $C_{33}H_{44}N_4 \cdot Cl_4O_2Pd_2$. Calculated, %: C 44.8; H 5.0; N 6.3.

Tetrachloro-μ-(4,4′-methylenebis{*N*-[(1*S*,3*S*,4*E*,6*R*)-4-hydroxyiminocaran-3-yl]aniline}-*N*,*N*,*N*′,*N*′)dicopper(II) $Cu_2(H_2L^2)Cl_4$ (II). A solution of 0.034 g (0.2 mmol) of $CuCl_2 \cdot 2H_2O$ in 1.5 ml of EtOH was added to a warm (~50–60°C) solution of 0.053 g (0.1 mmol) of H_2L^2 in 1.5 ml of EtOH. A solid gradually separated from the mixture. The mixture was kept for 7 days in a capped beaker at room temperature, and the dark green product was filtered off with suction, washed with EtOH and hexane and dried in air. Yield 0.052 g (60%). Found, %: C 49.5; H 5.6; N 7.0. $C_{33}H_{44}N_4Cl_4Cu_2O_2$. Calculated, %: C 49.7; H 5.5; N 7.0.

Tetrachloro-μ-(4,4′-methylenebis{*N*-[(1*S*,2*E*,4*R*)-2-hydroxyimino-*p*-menth-8-en-1-yl]aniline}- *N*,*N*,*N*′,*N*′)-dipalladium(II) $Pd_2(H_2L^3)Cl_4$ (III). A solution of 0.053 g (0.1 mmol) of H_2L^3 in 5 ml of a 1:1 (v/v) EtOH–MeCN mixture was added to a warm (~50–60°C) solution of 0.036 g (0.2 mmol) of $PdCl_2$ in a mixture of 2 ml of EtOH and 0.5 ml of concentrated hydrochloric acid. The resulting solution was filtered through a filter paper, and the filtrate was kept at room temperature. Fine orange solid gradually separated. The mixture was evaporated to a volume of ~2–3 ml, and the precipitate was filtered off with suction, washed with hexane, and dried in a vacuum desiccator. Yield 0.061 g (69%). $[\alpha]_{578}^{30}$ = +139 (*c* = 0.26, MeOH). Found, %: C 43.5; H 5.3; N 6.1. $C_{33}H_{44}N_4Cl_4O_2Pd_2$. Calculated, %: C 44.9; H 5.0; N 6.3.

Tetrachloro-μ-(4,4′-methylenebis{*N*-[(1*S*,2*E*,4*R*)-2-hydroxyimino-*p*-menth-8-en-1-yl]aniline *N*,*N*,*N*′,*N*′}-dicopper(II) $Cu_2(H_2L^3)Cl_4$ (IV). A solution of 0.034 g (0.2 mmol) of $CuCl_2 \cdot 2H_2O$ in 3 ml of MeCN was added to a solution of 0.053 g (0.1 mmol) of H_2L^3 in 4 ml of a 1:1 (v/v) *i*-PrOH–MeCN mixture. The resulting solution was kept at room temperature, and evaporation of the solvent was accompanied by gradual separation of dark green crystals. The solvent was evaporated to as small volume as possible (~2–3 ml), and the precipitate was filtered off with suction, washed with cold isopropyl alcohol and hexane, and dried in a vacuum desiccator. Yield 0.048 g (60%). Found, %: C 48.4; H 5.8; N 7.1. $C_{33}H_{44}N_4Cl_4Cu_2O_2$. Calculated, %: C 49.7; H 5.5; N 7.0.

A solution of 0.017 g (0.1 mmol) of $CuCl_2 \cdot 2H_2O$ in 3 ml of MeCN was added to a solution of 0.026 g (0.05 mmol) of H_2L^3 in 4 ml of a 1:1 (v/v) *i*-PrOH–MeCN mixture. While keeping the resulting solution at ~3°C single crystals of $[Cu(i\text{-}PrOH)Cl_2(\mu\text{-}H_2L^3)CuCl_2 \cdot H_2O]$ (**V**) separated and were withdrawn from the solution and covered with mineral oil.

ACKNOWLEDGMENTS

The authors thank V.A. Daletskii for measuring static magnetic susceptibilities, A.P. Zubareva and O.S. Koshcheeva for performing elemental analyses, and N.I. Alferova for recording IR spectra. This study was performed under financial support by the Russian Foundation for Basic Research (project no. 10-03-00346).

REFERENCES

1. Von Zelewsky, A. and Mamula, O., *J. Chem. Soc., Dalton Trans*., 2000, no. 3, p. 219.
2. Mamula, O. and von Zelewsky, A., *Coord. Chem. Rev*., 2003, vol. 242, p. 87.
3. Tkachev, A.V., *Ros. Khim. Zh*., 1998, vol. 42, nos. 1–2, p. 42.
4. Larionov, S.V. and Tkachev, A.V., *Ros. Khim. Zh*., 2004, vol. 48, no. 4, p. 154.
5. Larionov, S.V., Myachina, L.I., Glinskaya, L.A., Klevtsova, R.F., Sheludyakova, L.A., Tkachev, A.V., and Bizyaev, S.N., *Koord. Khim*., 2003, vol. 29, no. 12, p. 897.
6. Larionov, S.V., Myachina, L.I., Sheludyakova, L.A., Boguslavskii, E.G., Tkachev, A.V., and Bizyaev, S.N., *Koord. Khim*., 2004, vol. 30, no. 12, p. 897.
7. Larionov, S.V., Myachina, L.I., Savel'eva, Z.A., Glinskaya, L.A., Klevtsova, R.F., Sheludyakova, L.A., Tkachev, A.V., and Bizyaev, S.N., *Koord. Khim*., 2004, vol. 30, no. 12, p. 888.
8. Larionov, S.V., Savel'eva, Z.A., Glinskaya, L.A., Klevtsova, R.F., Bizyaev, S.N., and Tkachev, A.V., *Zh. Strukt. Khim*., 2005, vol. 46, no. 3, p. 558.

9. Larionov, S.V., Tkachev, A.V., Savel'eva, Z.A., Myachina, L.I., Glinskaya, L.A., Klevtsova, R.F., and Bizyaev, S.N., *Koord. Khim*., 2006, vol. 32, no. 4, p. 261.
10. Larionov, S.V., Savel'eva, Z.A., Glinskaya, L.A., Klevtsova, R.F., Sheludyakova, L.A., Bizyaev, S.N., and Tkachev, A.V., *Koord. Khim*., 2006, vol. 32, no. 5, p. 365.
11. Savel'eva, Z.A., Bizyaev, S.N., Glinskaya, L.A., Klevtsova, R.F., Tkachev, A.V., and Larionov, S.V., *Koord. Khim*., 2006, vol. 32, no. 10, p. 754.
12. Savel'eva, Z.A., Klevtsova, R.F., Glinskaya, L.A., Ikorskii, V.N., Bizyaev, S.N., Tkachev, A.V., and Larionov, S.V., *Koord. Khim*., 2006, vol. 32, no. 11, p. 816.
13. Larionov, S.V., Kokina, T.E., Agafontsev, A.M., Gorshkov, N.B., Tkachev, A.V., Klevtsova, R.F., and Glinskaya, L.A., *Koord. Khim*., 2007, vol. 33, no. 7, p. 525.
14. Kokina, T.E., Myachina, L.I., Glinskaya, L.A., Tkachev, A.V., Klevtsova, R.F., Sheludyakova, L.A., Bizyaev, S.N., Agafontsev, A.M., Gorshkov, S.N., and Larionov, S.V., *Koord. Khim*., 2008, vol. 34, no. 2, p. 120.
15. Larionov, S.V., Tkachev, A.V., Myachina, L.I., Savel'eva, Z.A., Glinskaya, L.A., Klevtsova, R.F., Agafontsev, A.M., and Bizyaev, S.N., *Koord. Khim*., 2009, vol. 35, no. 4, p. 291.
16. Tkachev, A.V., Petukhov, P.A., Konchenko, S.N., Korenev, S.V., Fedotov, M.A., Gatilov, Yu.V., Rybalova, T.V., and Kholdeeva, O.A., *Tetrahedron: Asymmetry*, 1995, vol. 6, no. 1, p. 115.
17. Larionov, S.V., Myachina, L.I., Tkachev, A.V., Sheludyakova, L.A., and Boguslavskii, E.G., *Koord. Khim*., 2002, vol. 28, no. 12, p. 909.
18. Larionov, S.V., Myachina, L.I., Glinskaya, L.A., Klevtsova, R.F., Bizyaev, S.N., and Tkachev, A.V., *Izv. Akad. Nauk, Ser. Khim*., 2007, no. 9, p. 1708.
19. Larionov, S.V., Savel'eva, Z.A., Glinskaya, L.A., Klevtsova, R.F., Ikorskii, V.N., Bizyaev, S.N., and Tkachev, A.V., *Zh. Neorg. Khim*., 2005, vol. 50, no. 5, p. 786.
20. Tkachev, A.V., Denisov, A.Yu., Rukavishnikov, A.V., Chibirjaev, A.M., Gatilov, Yu.V., and Bagrjanskaja, I.Yu., *Aust. J. Chem*., 1992, vol. 45, no. 6, p. 1077.
21. Larionov, S.V., Savel'eva, Z.A., Romanenko, G.V., Tkachev, A.V., Ikorskii, V.N., and Boguslavskii, E.G., *Koord. Khim*., 2002, vol. 28, no. 11, p. 832.
22. Kokina, T.E., Glinskaya, L.A., Klevtsova, R.F., Boguslavskii, E.G., Sheludyakova, L.A., Bizyaev, S.N., Tkachev, A.V., and Larionov, S.V., *Koord. Khim*., 2009, vol. 35, no. 3, p. 202.
23. Savel'eva, Z.A., Tkachev, A.V., Glinskaya, L.A., Bizyaev, S.N., Klevtsova, R.F., and Larionov, S.V., *Koord. Khim*., 2009, vol. 35, no. 2, p. 130.
24. Myachina, L.I., Tkachev, A.V., Romanenko, G.V., Sheludyakova, L.A., Boguslavskii, E.G., and Larionov, S.V., *Koord. Khim*., 2003, vol. 29, no. 8, p. 611.
25. Mishra, A.K., Purohit, C.S., and Verma, S., *Cryst. Eng. Commun*., 2008, vol. 10, no. 10, p. 1296.
26. Higgins, S.J. and Shaw, B.L., *J. Chem. Soc., Dalton Trans*., 1988, no. 2, p. 457.
27. Petukhov, P.A., Bizyaev, S.N., and Tkachev, A.V., *Izv. Akad. Nauk, Ser. Khim*., 2001, no. 11, p. 2013.
28. Sheldrick, G.M., *SHELXS97 and SHELXL97. Programs for the Refinement of Crystal Strustures*, Göttingen (Germany): Univ. of Göttingen, 1997.